CONDITIONS AND LIMITATIONS FOR RESOLUTION OF HYPERFINE STRUCTURE IN THE AUTLER-TOWNES SPECTRA

T. Kirova[1], A. Ekers[1], N. N. Bezuglov[2], I. I. Ryabtsev[3], M. Auzinsh[1], K. Blushs[1]

[1] *Laser Centre, University of Latvia, Riga, Latvia*

[2] *Faculty of Physics, St. Petersburg State University, St. Petersburg, Russia*

[3] *Department of Quantum Electronics, Institute of Semiconductor Physics, Novosibirsk, Russia*

Results of preliminary simulations of Autler-Townes effect in atomic and molecular level systems with hyperfine structure are presented. A system of three states with hyperfine structure in Na and Na_2 coupled in a ladder linkage scheme by a weak probe field and a strong coupling field is studied by solving the density matrix equations of motion. The simulations show that application of a strong coupling field to systems with large hyperfine level splittings leads to a full resolution of M_F Zeeman sublevels of the hyperfine levels F. This resolution improves as the coupling field Rabi frequency is increased to values much larger than the hyperfine level separations. In molecules, where hyperfine splittings are very small, the M_F Zeeman sublevels can only be resolved at very small coupling field strengths and only if the HF splittings are larger than the natural widths of excited states and the laser linewidths. When the coupling field Rabi frequency exceeds the hyperfine level separations, the M_F resolution is completely lost. This effect is interpreted in terms of the formation of dark states when a number of closely lying energy levels are coupled by a strong field to another energy level.

I. Introduction.

Recent advances in quantum optics have led to the discovery of many novel and intriguing phenomena such as electromagnetically induced transparency (EIT) [1], narrowing of spectral lines [2], and lasing without inversion (LWI) [3]. The underlying effect in all of them is the destructive quantum interference between different excitation pathways leading to reduction or full cancellation of transition probabilities. The first coherent interference experiment showing cancellation of absorption was performed by Fano [4] and subsequently led the idea of coherent population trapping (CPT) [5]. In a typical lambda scheme, a certain ratio of the applied field strengths leads to the creation of a 'dark' state.

Taichenachev *et al.* [6] have obtained analytical expressions for dark resonance line shapes, where the full atomic structure, including magnetic and hyperfine levels, is included. Hioe and Carroll [7] investigated the behaviour of a multilevel quantum system interacting with a strong laser field and demonstrated the existence of different invariants (including CPT) depending on the number of levels N. Experimental observation of CPT in ^{87}Rb vapor cell was reported by Zhu *et al*. [8], where multilevel dark states were created between two or three out of five degenerate magnetic sublevels in one of the ground state hyperfine levels.

The above phenomena are related to the Autler-Townes (AT) effect [9]. While extensively studied in atoms [10], experiments in molecular systems are still relatively few [11]. The AT effect has a potential for new applications to molecular spectroscopy, like measurement of the transition dipole moments [11a-d] and lifetimes of highly excited molecular states using cw laser fields [11d], and all-optical alignment of non-polar molecules [11c].

McClean and Swain [12] discussed that the three-level resonant model of Feneuille and Schweinhofer [13] can not adequately describe the AT splitting experiment of Pique and Pinard [10a] in Na atoms. They investigated the effect of non-resonant neighboring hyperfine levels as well as the role of magnetic sublevel degeneracy and concluded that both can significantly modify the population of the upper level, especially at high laser intensities.

The present study is focused on effects of hyperfine structure on the AT effect. We consider ladder systems of hyperfine levels F in Na atoms and Na_2 molecules (see Fig. 1), each of which is $2F+1$-fold degenerate over the magnetic number M_F. Of special concern is determination and interpretation of the conditions under which the hyperfine interaction becomes negligible. An intuitive assumption would be that the coupling of hyperfine components by the laser field depends on the hyperfine and magnetic quantum numbers, which would lead to a different AT splittings different M_F components. The calculations show, however, that systems wit large and small hyperfine splittings actually respond differently to coupling by strong laser fields.

II. Large HF splitting

II.A. Excitation scheme in Na atoms

Lagrge HF splittings are usually observed in low-lying energy levels of atoms. We consider a ladder scheme of three atomic states in Na, where each state has a well resolved hyperfine structure (Fig. 1a). A weak probe laser P excites the atoms from the ground state $|g\rangle$ ($3S_{1/2}$, F_g =1, 2) to the intermediate state $|e\rangle$ ($3P_{1/2}$ state, F_e =1, 2), which is further coupled by a strong laser field S to the final state $|f\rangle$ ($5S_{1/2}$, F_f =1, 2). Unless specified otherwise, the laser linewidth is assumed to be 1MHz. Both laser fields are linearly polarised, which implies the selection rule $\Delta M_F = 0$ for laser-driven

transitions. The transition dipole matrix element between two M_F magnetic sublevels of two hyperfine F states can be evaluated as [16]

$$\left\langle F_f M_{F_f} \left| \mu_q \right| F_e M_{F_e} \right\rangle = (-1)^{F_f - M_{F_f}} \begin{pmatrix} F_f & 1 & F_e \\ -M_{F_f} & q & M_{F_e} \end{pmatrix} \times (-1)^{F_f + I + J_e + 1} \sqrt{(2F_e + 1)(2F_f + 1)} \begin{Bmatrix} J_e & F_e & I \\ F_f & J_f & 1 \end{Bmatrix} (J_f \| \mu \| J_e), \quad (1)$$

where $(J_f \| \mu \| J_e)$ is the reduced matrix element, and () and {} brackets represent the 3j and 6j symbols, respectively. Since the Rabi frequency of the strong coupling field is proportional to (1), the F and M_F dependence transfers to the splitting of the AT doublet. Therefore, we expect the excitation spectrum of levels |*e*> and |*f*> to consist of a number of AT split peaks, associated with each hyperfine and magnetic sublevel components.

II.B. Theoretical model

The optical Bloch equations (OBEs) for the density matrix are given by

$$\frac{d\rho}{dt} = -\frac{i}{\hbar}\left[\hat{H}, \rho\right] + \hat{R}\rho, \quad (2)$$

where the total Hamiltonian $\hat{H}$ of the atom-laser system includes the unperturbed atomic Hamiltonian as well as the dipole interaction operator $\hat{V} = -\hat{\vec{\mu}} \cdot \vec{E}$. The relaxation term $\hat{R}$ accounts for relaxation due to spontaneous emission and transit relaxation of the molecules through the laser beam. Equation (2) results in a system of OBEs for Zeeman coherences $\rho_{g_i g_j}, \rho_{e_i e_j}, \rho_{f_i f_j}$ and optical coherences $\rho_{g_i e_j}, \rho_{e_i g_j}, \rho_{e_i f_j}, \rho_{f_i e_j}$. The solution of this system yields populations of levels |*g*>, |*e*>, and |*f*>. For a full description of the model see [17].

II.C. Numerical Results for Atoms

We perform numerical simulations based on the OBEs model including the interaction of both laser fields with all the hyperfine levels in the system. Doppler broadening is not taken into account. Figure 2 shows the $|f\rangle$ state population as a function of probe field detuning for four different values of the coupling field Rabi frequency. At low intensity of the coupling field (Fig. 2a) the spectrum consists of two pairs of peaks which correspond to two-photon (one from the probe filed and one from the coupling field) excitation from the two ground state hyperfine levels to the two hyperfine components of level $|f\rangle$. With the increase of the coupling field Rabi frequency, a separation of the Zeeman components M_F is seen (Figs. 2b and 2c) until their full resolution at Ω_S=2GHz (Fig. 2d). In the latter case the coupling field Rabi frequency exceeds the hyperfine splittings of both the $3P_{1/2}$ state ($\Delta E_{F=1,F=2}$=188.88 MHz) and the $5S_{1/2}$ state ($\Delta E_{F=1,F=2}$=156 MHz) by more than ten times. The number of hyperfine components in the AT spectrum is in accordance with the number of possible couplings of M_F sublevels in levels |g>, |e> and |f>, which are subject to the selection rule $\Delta M_F = 0$ and an additional restriction of the $M_{F'}=0 \rightarrow M_F = 0$ transition if $F' = F$.

It is instructive to see what would happen in the case of smaller HF splittings. For the sake of simplicity we shall consider only the transition $F_g=1 \rightarrow |e\rangle \rightarrow |f\rangle$. Figure 3 shows the variation of the excitation spectrum of level $|f\rangle$ at Ω_S=2GHz as the hyperfine constant A_{hfs} of level $|f\rangle$ is reduced. The spectrum is initially splitted in two triplets at the original A_{hfs} = 78MHz (Fig. 3a). When A_{hfs} is reduced by a factor of two, the outermost components off each triplet remain at the same positions, while the middle ones are shifted towards the respective rhs outermost peaks (Fig. 3b). When A_{hfs} is reduced by a factor of 10, the middle peaks is shifted even more and cannot be resolved for the rhs peaks.

The above results are consistent with the reuslts obtained using a much simpler treatment of laser-atom system based on solving the Shrödinger's equation, which yiled the time evolution of the probability amplitudes in the atomic wavefunction. Comparison with the simulations obtained by both approaches (Fig.4) shows the same energy positions of the M_F Zeeman sublevels under the action of a strong laser field but different widths and intensities of the AT peaks, since no cascading due to spontaneous emission is included in Shrödinger's equation.

III. Small HF splitting

III.A. Excitation Scheme in Molecules

Small HF splittings of energy levels are characteristic to molecules. We consider a ladder of three rovibronic levels in Na with hyperfine structure (Fig. 1b), where state $|g\rangle$ is the $X^1\Sigma^+_g$ (J=1) state, state $|e\rangle$ is the $A^1\Sigma^+_u$ (J=0) state and $5^1\Sigma^+_g$ (J=1) represents the final state $|f\rangle$. The hyperfine splittings are of an order of $10^{-1}\div10^2$ kHz, which is well bellow the natural widths of levels $|e\rangle$ and $|f\rangle$.

The nucleus of the sodium ^{23}Na atom has a spin of 3/2, which leads to a total nuclear spin of I =3, 2, 1, or 0 for the sodium molecule. Since the atomic nucleus obeys the Fermi statistics, the total molecular wave function has to be anti-symmetric, e.g. symmetric rotational levels must have anti-symmetric nuclear spin functions, and vice versa. This leads to certain restrictions on the values of I for the chosen rotational levels. For the $X^1\Sigma^+_g$ (J=1) and $5^1\Sigma^+_g$ (J=1) states the possible values of the total nuclear spin and hyperfine number are I=0, F=2, 1, 0 or I=3, F=4, 3, 2. For the $A^1\Sigma^+_u$ (J=0) state I=0, F=1 or I=3, F=3. Since ΔI=0 selection rule holds for transitions between hyperfine levels, we consider only excitations between levels with I=3 for simplicity.

III.B. Numerical Results for Molecules

The final state population calculated with OBEs model as a function of the probe laser detuning for a value Ω_S=500 MHz is given in Fig.5. Figures 5a-c show the full resolution of the magnetic sublevels M_F when only one hyperfine level F_f =2, 3 or 4 in the final state is considered. However, the inclusion of more than one hyperfine level in the final state leads to a complete loss of the M_F structure (Fig.5d); the states behave as J levels with M_J sublevels with no hyperfine structure.

Similar results are obtained if narrow laser linewidths (1 Hz) and long lifetimes of excited states (τ = 100 μs) are used. If the Rabi frequencies are smaller than the HF splittings, then the HF structure is well resolved in the excitation spectrum of the upper level (Fig. 6a). If the Rabi frequency of the strong coupling field is increased, some of the HF components lose intensity (Fig. 6b), while at large intensities (Fig. 6c) the spectrum looks basically the same as in Fig. 5d.

The latter is an interesting observation which contrasts with the behaviour of dressed levels in the case of large HF splittings. When the HF splitting is large, then increased Rabi frequency of the strong coupling field leads to a better resolution of the multitude of dressed states built of different HF levels. When the HF splitting is small, then increased Rabi frequency of the strong coupling field leads to a complete disappearance of the HF structure.

IV. Creation of Multiple Dark States

In order to understand the above effects, we applied the Shrödinger's equation method for the model excitation scheme shown in Fig. 7, where the final state consists of six closely spaced levels separated by Δ = 100 KHz. As can be seen from Figs.8 a-d, the increase of the coupling field strength Ω_S compared to values larger than the

separation Δ between the final states leads to a gradual decrease (Figs. 8a-c) and eventually vanishing (Fig. 8d) of the intensity of all AT peaks except the two outer ones.

The above effect can be interpreted by examining the dressed-states approach. Consider the situation when a molecular quantum state $|\psi_0\rangle$ is coupled with a system of quantum states $|\psi_n\rangle$ by the laser field E_S as it is depicted on Fig 9a. The corresponding Rabi frequency $\Omega_n = \langle\psi_n|E_S|\psi_0\rangle$ may have arbitrary values. Our aim is to find a set of dressed states. In the rotating wave approximation the coupling diagram can de depicted as in Fig. 9b. The total Hamiltonian $\hat{H} = \hat{H}_0 + \hat{E}_S$ of such a system has the form

$$\hat{H}\begin{pmatrix} C_0 \\ C_1 \\ . \\ . \\ C_{n-1} \\ C_n \end{pmatrix} = \frac{\hbar}{2}\begin{bmatrix} 0 & \Omega_1 & . & . & \Omega_{n-1} & \Omega_n \\ \Omega_1 & \Delta_1 & . & . & 0 & 0 \\ . & . & . & . & . & . \\ . & . & . & . & . & . \\ \Omega_{n-1} & 0 & . & . & \Delta_{n-1} & 0 \\ \Omega_n & 0 & . & . & 0 & \Delta_n \end{bmatrix}\begin{pmatrix} C_0 \\ C_1 \\ . \\ . \\ C_{n-1} \\ C_n \end{pmatrix}, \qquad (3)$$

which is in the basis of the bare states ψ_i $(i = 0,1,..,n)$,

$$\psi(t) = \exp(-i\omega_S t - i\varepsilon_0 t/\hbar)\sum_{i\neq 0} C_i(t)\psi_i + \exp(-i\varepsilon_0 t/\hbar)C_0(t)\psi_0 \qquad (4)$$

The Hamiltonian $\hat{H}_0$ corresponds to a free molecule and determines the bare state energies $\Delta_i = \varepsilon_i/\hbar - (\omega_S + \varepsilon_0/\hbar)$ $(i \neq 0)$. The value Δ_0 for the low-lying state $i = 0$ is chosen as zero. The values of Δ_i correspond to the diagonal elements and given by laser detunings from resonance frequencies $(\varepsilon_i - \varepsilon_0)/\hbar - \omega_S$ of the corresponding optical transitions. The Rabi frequencies Ω_n give nondiagonal matrix elements and are determined with the coupling term $\hat{E}_S$ of the Hamiltonian $\hat{H}$.

In order to diagonalize the coupling part $\hat{E}_S$, we shall first find all solutions $\psi_D = \sum_{i\neq 0} C_i^{(D)} \psi_i$ of the equation

$$\langle \psi_0 | E_S | \psi_D \rangle = 0 \tag{5}$$

Importantly, the wave function ψ_D does not contain $|\psi_0\rangle$. Obviously, ψ_D is not involved in the laser-system interaction (see Fig. 9c); hence, it is a dark state. The coefficients $C_i^{(D)}$ obey a simple relation $\sum_{i\neq 0} C_i^{(D)} \Omega_i = 0$. It is convenient to rewrite it as

$$\langle \psi_B | \hat{I} | \psi_D \rangle = 0; \qquad |\psi_B\rangle = \frac{1}{\sqrt{\sum_{i\neq 0} \Omega_i^2}} \sum_{i\neq 0} \Omega_i \psi_i, \tag{6}$$

in which ψ_B and ψ_D are orthogional. Straightforward calculation yields

$$\langle \psi_0 | E_S | \psi_B \rangle \equiv \Omega_{eff} = \sqrt{\sum_{i\neq 0} \Omega_i^2}\ . \tag{7}$$

The function ψ_B is strongly coupled with the low-lying state with the effective Rabi frequency Ω_{eff} and may be considered as an analogue of a bright state.

Equation (6) implies that the subspace Λ_D, which includes the dark states, is orthogonal to the one-dimensional subspace containing the single bright state. In other words, the dimension of Λ_D is *n-1*, i.e., there are *n-1* dark states. The corresponding new diagram for the coupling matrix $\hat{E}_S$ is depicted in Fig. 8c. If the interaction is strong, i.e., if the separation between the bare state energies are negligible compared to the effective Rabi frequency

$$\Omega_{eff} >> \Delta_i \qquad (i = 1, ..., n), \tag{8}$$

then the subspace Λ_D is not excited by the laser field. Only the bright state is involved in the interaction with the low-lying states, which results in the formation of two dressed states $|+\rangle, |-\rangle$ with energies $\varepsilon_\pm$:

$$\hat{H}|\pm\rangle = \varepsilon_\pm |\pm\rangle; \quad \varepsilon_\pm = \frac{1}{2}\left[\Delta_B \pm \sqrt{\Delta_B^2 + \Omega_{eff}^2}\right]; \quad \Delta_B = \langle\psi_B|\hat{H}_0|\psi_B\rangle = \sum_{i\neq 0}\Omega_i^2\Delta_i / \sum_{i\neq 0}\Omega_i^2 .$$

In experiment, the situation depicted on Fig. 8c corresponds to the excitation of only two levels $\varepsilon_\pm$, i.e., only one doublet would appear in the excitation spectrum.

V. Conclusion

The simulations of Autler-Townes spectra for molecules with small hyperfine splittings of energy levels show that when a strong coupling field is used, the hyperfine structure cannot be resolved regardless if the splittings are smaller (Fig. 5d) or larger (Fig. 6c) than the natural widths of excited levels. The dressed state analysis leads to a conclusion that resolution of M_F Zeeman sublevels is not possible because of the formation of multiple dark states in a multilevel system coupled by laser field with Rabi frequency much larger than the level separation. It is, however, not yet quite clear why the M_F resolution is not lost in the atomic hyperfine level system, when the coupling Rabi frequency is much larger than the HF level separations (Fig2d). Further investigation of AT effect in level systems with hyperfine structure are in progress and will be reported elsewhere.

This work was funded by the EU FP6 TOK project LAMOL, Latvian Science Council, and UL project Y2-ZP-114-100. I.I.R. acknowledges support from RFBR grant No. 08-02-00220.

Figure Captions

Fig. 1: Excitation schemes in Na (frame (a)) and Na_2 (frame (b)).

Fig. 2: Population of level $|f\rangle$ vs probe field detuning for different S field Rabi frequencies. Simulations are performed using parameters Ω_p=1 MHz, transit relaxation of 1 MHz, laser linewidth of 1 MHz for both laser fields, and lifetimes of the $3P_{1/2}$ and $5S_{1/2}$ states of 16.35 ns and 77.6 ns, respectively.

Fig. 3: The F_g=1→$|e\rangle$→$|f\rangle$ component of the excitation spectrum in Fig. 2d for different values of A_{hfs}. Other simulation parameters are equal to those used in Fig. 2.

Fig. 4: Comparison of AT spectra obtained by the solution of OBEs and Schreodinger's equation. Simulation parameters are equal to those used for Fig. 2d.

Fig. 5: Population of level $|f\rangle$ vs probe field detuning calculated for each hyperfine component separately (frames (a), (b), and (c)) and for all components simultaneously (frame (d)). The simulations were performed with Ω_S=500 MHz, Ω_p=1 MHz, transit relaxation of 10 kHz, linewidths of both laser fields of 10 kHz, and lifetimes of the $A^1\Sigma^+_u$ and $5^1\Sigma^+_g$ states of 12.45 ns and 40 ns, respectively.

Fig. 6: (a), (b), (c) Write text for spectrum for molecules with long lifetimes and narrow laser linewidhs.

Fig. 7. Model system for state |*f*> consisting of six closely spaced levels |1>, …, |6> separated by Δ = 100 KHz and coupled by a strong laser filed E_S to level |e>, while levels |g> and |e> are coupled by a weak probe field E_P.

Fig. 8: Population of level |*f*> vs probe field detuning for different Rabi frequencies of coupling field: (a) Ω_S = 50KHz; (b) Ω_S = 100KHz; (c) Ω_S = 200KHz; (d) Ω_S = 400KHz. The simulations were performed with Ω_p = 1kHz, Δ=100kHz, and the decay rates of levels |e> and |f> of 10 kHz.

Fig. 9: (a) Coupling scheme of bare states. (b) Coupling diagram in the rotating wave approximation; (c) the coupling diagram can de depicted as in Fig. 9b.

(c) Coupling of the lower state $|\psi_0\rangle$ and the bright state $|\psi_B\rangle$ to the dressed states |–> and |+>; dark states ψ_D from subspace Λ_D are not involved in coupling.

References

[1]Harris, S. E., Field, J. E., and Imamoglu, A., Phys. Rev. Lett. **64**, 1107 (1990); Harris, S. E., Phys. Today **50**, 36 (1997)

[2] Narducci, L. M., Scully, M. O., Oppo, G. -L.,*et al.*, Phys. Rev. A **42**, 1630 (1990); Manka, A. S., Doss, H. M., Narducci, L. M., *et al.*, Phys. Rev. A **43**, 3748 (1991); Zhou, P., and Swain, S., Phys. Rev. Lett. **77,** 3995 (1996)

[3] Kocharovskaya, O., and Khanin, Ya. I., Pi'sma Zh. Eksp. Teor. Fiz. **48**, 581(1988) (JETP Lett.48, 630 (1988));Harris, S. E., Phys. Rev. Lett. **62**, 1033 (1989)

[4] Fano, U., Phys. Rev. **124** , 1866 (1961)

[5]Alzetta, G., Gozzini, L., Moi, L., and Orriols, G., Il Nuovo Cimento **36B**, 5 (1976); Arimondo, E. and Orriols, G., Lettere al Nuovo Cimento **17**, 333 (1976)

[6] Taichenachev, A. V., Yudin,V. I., Wynands, R., *et al.* Phys. Rev. A. **67**, 033810 (2003)

[7] Hioe, F.T. and Carroll,C. E., Phys. Rev. A. **37,** 3000 (1988)

[8] Zhu, Y., Wang, S., and Mulchan, N. M., Phys. Rev. A. **59**, 4005 (1999)

[9] Autler, S. H. and Townes, C. H., Phys. Rev. **100**, 703 (1955)

[10] Picque, J. L. and Pinard, J., J. Phys. B: At. Mol. Phys. **9**, L77 (1976 ; Delsart, C. and Keller, J.–C., J. Phys. B: At. Mol. Phys. **9**, 2769 (1976); Gray, H. R. and Stroud, C. R., Opt. Commun. **25**, 359 (1978); Knight, P. L. and Milonni, P. W., Phys. Rep. 66, 21 (1980)

[11] a)Quesada, M. A., Lau, A. M. F., Parker, D. H., and Chandler, D. W., Phys. Rev. A, **36**, 4107 (1987); b) Qi, J., Spano, F.C., Kirova, T. *et al*., Phys. Rev. Lett., **88**, 173003 (2002); c) Qi, J. , Lazarov, G., Wang, X., *et al*., Phys. Rev. Lett., **83**, 288 (1999) ; d) Garcia-Fernandez, R., Ekers, A., Klavins, J., *et al*., Phys. Rev. A, **71**, 023401 (2005) ; e) Atherton, P. S., Dalton, B. J., and Dagg, I. R., J. Phys. B: At. Mol. Phys. **19**, 277 (1986)

[12] McClean, W. A. And Swain, S., J. Phys. B: At. Mol. Phys. **10**, L143 (1977)

[13] Feneuille. S. and Schweighofer, M. -G., J. Physique **36**, 781 (1975)

[14] Sussman, B. J., Ivanov, M. Yu., and Stolow, A., Phys. Rev. A **71**, 051401 (2005); Sussman, B. J., Underwood, J. G., Lausten, R., *et al.* Phys. Rev. A **73**, 053403 (2006)

[15]Wollenhaupt, M., Prakelt, A., Sarpe-Tudoran, C., *et al.*, J. Opt. B **7**, S270 (2005); Wollenhaupt, M., Liese, D., Prakelt, A., *et al.,* Chem. Phys. Lett. **419**, 184 (2005); Wollenhaupt, M., Prakelt, A., Sarpe-Tudoran, C., *et al.,* Phys. Rev. A **73**, 063409 (2006)

[16]Zare, R. N., 1986, *Angular Momentum,* (Wiley-Interscience, New York)

[27]Auzinsh, M., Blushs, K., Ferber, R., *et al*. Opt. Commun. **264**, 333 (2006)

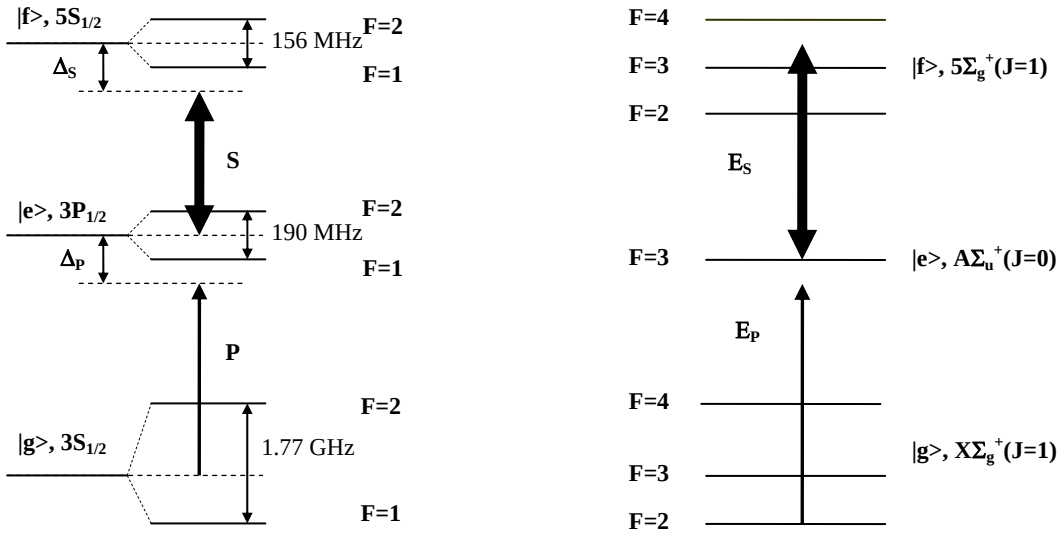
|f>, 5S1/2
156 MHz
F=2
F=1
ΔS
S
|e>, 3P1/2
F=2
190 MHz
ΔP
F=1
P
F=2
|g>, 3S1/2
1.77 GHz
F=1
F=4
F=3
|f>, 5Σg+(J=1)
F=2
ES
F=3
|e>, AΣu+(J=0)
EP
F=4
|g>, XΣg+(J=1)
F=3
F=2

(a) (b)

Fig. 1.

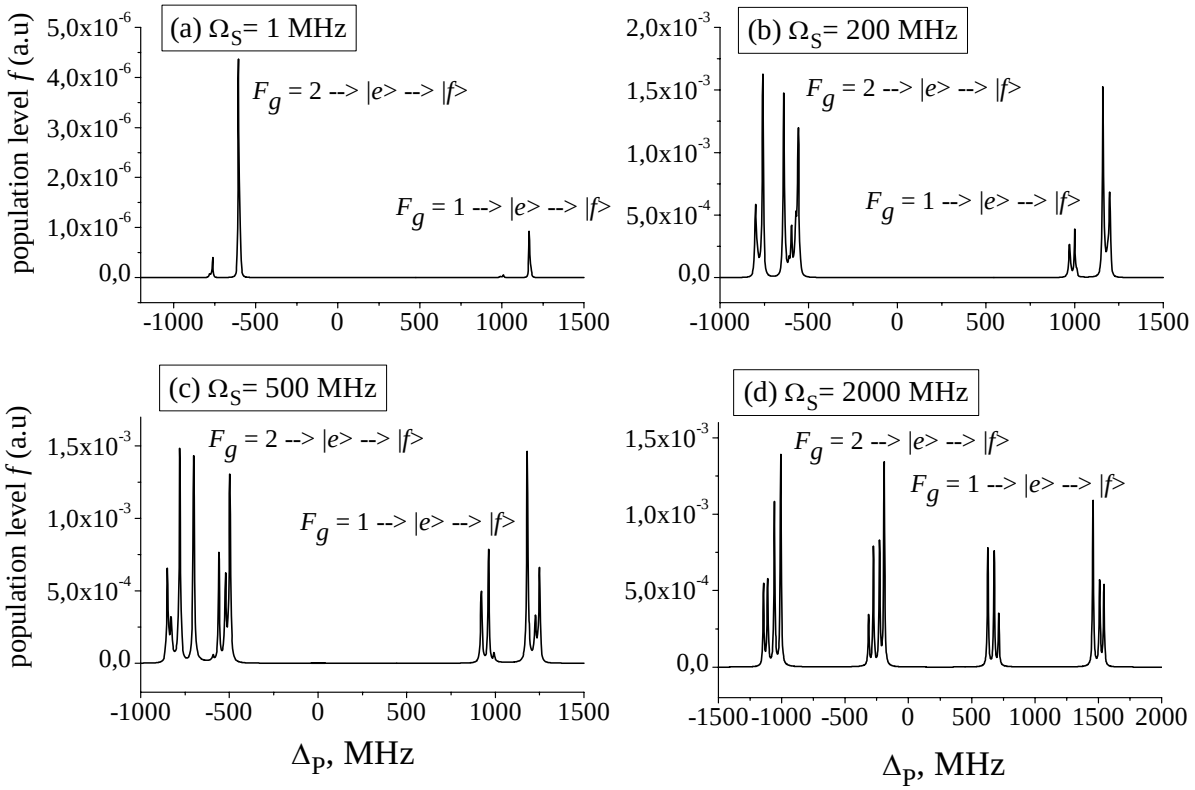
(a) Ω_S= 1 MHz
(b) Ω_S= 200 MHz
(c) Ω_S= 500 MHz
(d) Ω_S= 2000 MHz
F_g = 2 --> |e> --> |f>
F_g = 1 --> |e> --> |f>
population level f (a.u)
Δ_P, MHz

Fig. 2.

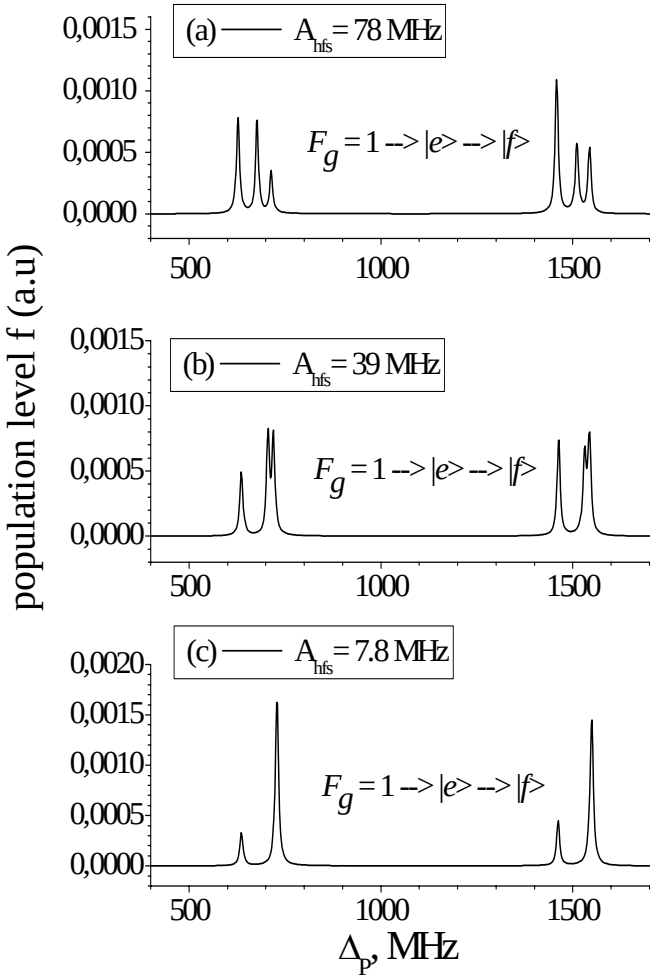
(a) —— A_hfs = 78 MHz
F_g = 1 --> |e> --> |f>
(b) —— A_hfs = 39 MHz
F_g = 1 --> |e> --> |f>
(c) —— A_hfs = 7.8 MHz
F_g = 1 --> |e> --> |f>
population level f (a.u)
Δ_p, MHz
0,0015
0,0010
0,0005
0,0000
0,0020
500
1000
1500

Fig. 3.

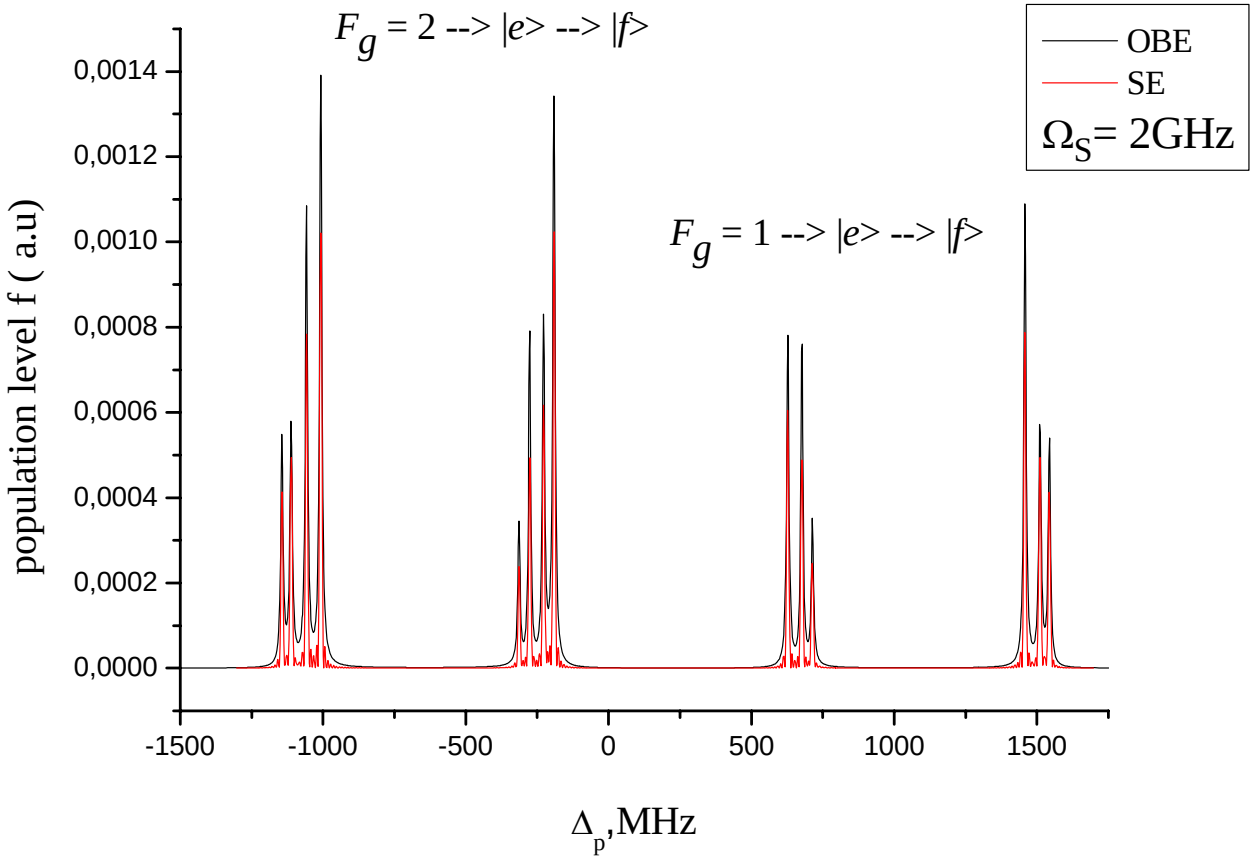
F_g = 2 --> |e> --> |f>
F_g = 1 --> |e> --> |f>
OBE
SE
Ω_S= 2GHz
population level f (a.u)
0,0014
0,0012
0,0010
0,0008
0,0006
0,0004
0,0002
0,0000
-1500
-1000
-500
0
500
1000
1500
Δ_p,MHz

Fig. 4.

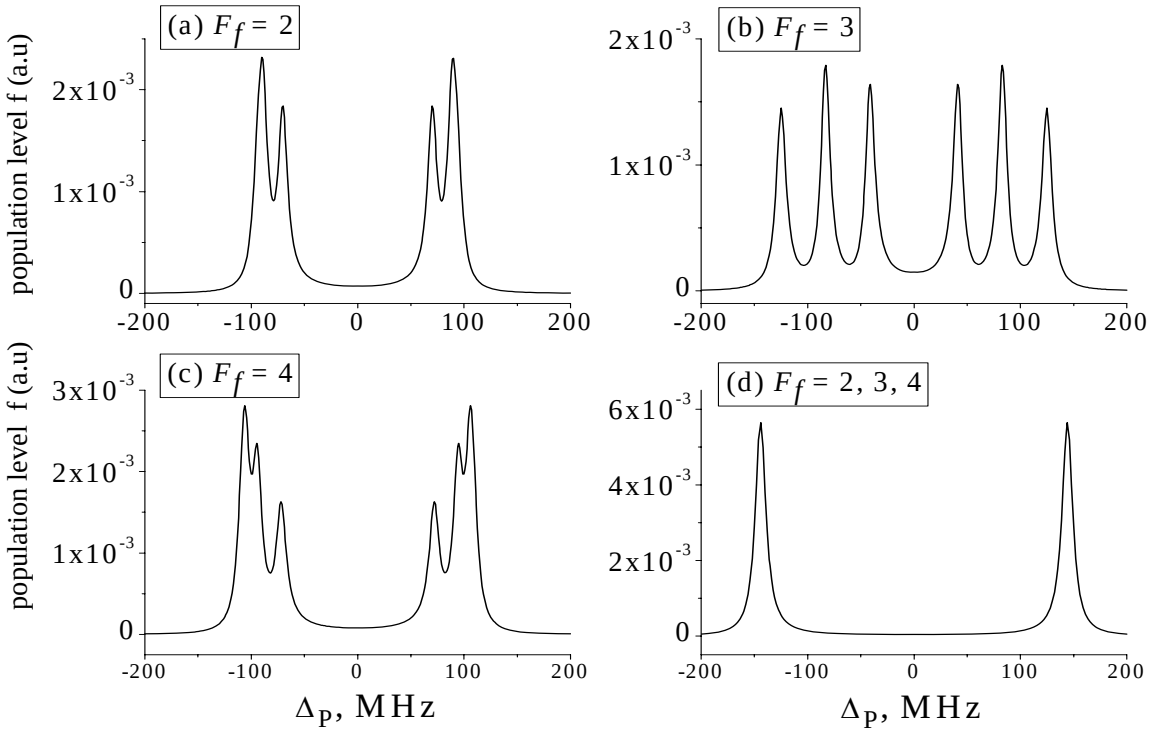
(a) F_f = 2
(b) F_f = 3
(c) F_f = 4
(d) F_f = 2, 3, 4
population level f (a.u)
population level f (a.u)
2x10-3
1x10-3
0
3x10-3
6x10-3
4x10-3
-200
-100
0
100
200
Δ_p, MHz
Δ_p, MHz

Fig. 5.

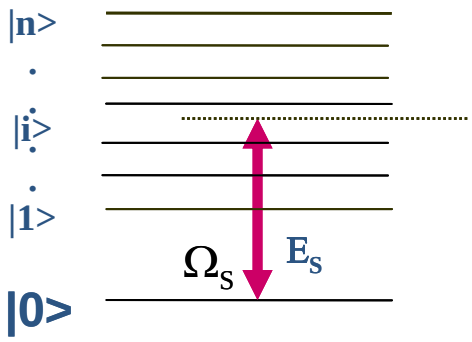

(a)

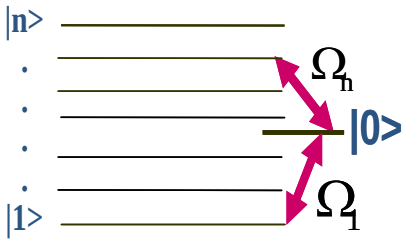

(b)

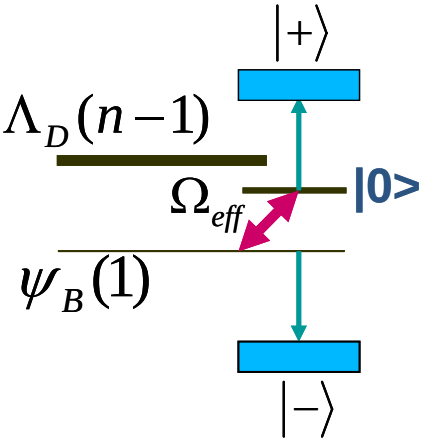

(c)

Fig. 6.

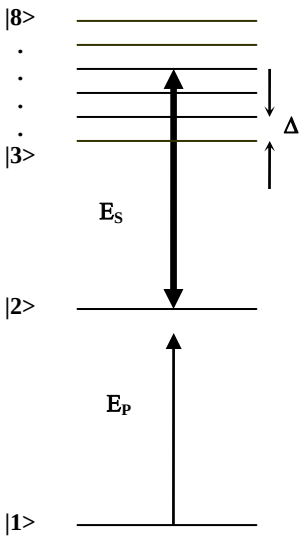
|8>
|3>
Δ
E_S
|2>
E_P
|1>

Fig. 7.

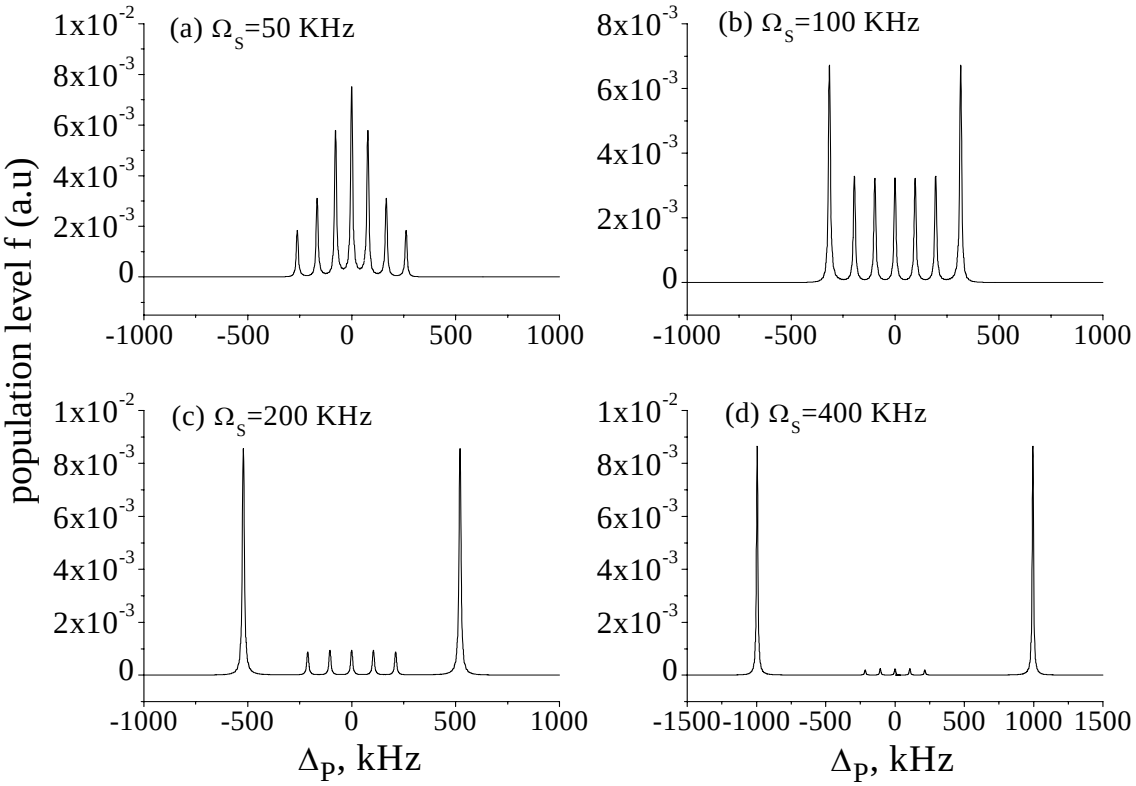
population level f (a.u)
(a) Ω_S=50 KHz
(b) Ω_S=100 KHz
(c) Ω_S=200 KHz
(d) Ω_S=400 KHz
1x10^-2
8x10^-3
6x10^-3
4x10^-3
2x10^-3
0
-1000
-500
0
500
1000
-1500
1500
Δ_P, kHz